Seismic Theory III: Discrete Grid Methods

Wednesday Morning, October 28th

High-Order Spectral Element Method for Elastic Wave Modeling

ST3.1

Geza Seriani, Enrico Priolo, Jose Carcione, and Enrico Padovani, Osservatorio Geofisica Sperimentale, Italy*

Summary

This work develops the Spectral Element Method (SPEM) for the solution of the two-dimensional elastic wave equation. The advantages of SPEM compared to low-order finite elements is the high accuracy, and the possibility of using less grid points per minimum wavelength. In addition, SPEM is more flexible than conventional finite differences and pseudospectral methods for describing problems with complex geometries; irregular surfaces between different media can be defined with great accuracy and boundary conditions can be easily implemented. The algorithm is tested against the analytical solution in a two-dimensional homogeneous medium, and numerical simulations through a steplike surface layer overlying a half space are computed.

Introduction

The Spectral Element Method is a high-order finite element technique and for this reason it is a particular case of the class of discrete numerical techniques for solving differential equations, known as the method of weighted residuals (MWR). Its distinguishing feature is that the computational domain is build up using a tensor product of high-order orthogonal functions. In this way, the method combines the characteristics of both spectral and finite element methods. In particular, interface problems are easily and accurately described. With the MWR, the solution of a problem is computed by solving an equivalent variational form i.e., by minimizing a residual with respect to a suitable norm. The residual is usually computed as the error produced in the differential equation when a truncated expansion is used instead of the exact solution. To this end, a set of trial functions and a set of weight functions must be defined. The trial functions are used as the basis functions for the truncated series expansion of the solution, while the weight functions are used to ensure that the differential equation is satisfied as closely as possible by the truncated series expansion. In the case of finite element methods, the trial functions are build up as a sum of functions with local support, and thus they are well suited for handling complex geometries (Hughes, 1987). Following the Galerkin approach, the weight functions can be the same as the trial functions and are, therefore, smooth functions which individually satisfy the boundary conditions.

The Chebyshev SPEM is based on the idea of decomposing the computational domain into rectangular subdomains, and then, on each subdomain expressing the solution of the variational problem by a truncated expansion of Chebyshev orthogonal polynomials (Patera, 1984).

In previous works, Priolo and Seriani (1991) and Seriani and Priolo (1991) have developed and investigated the method for the acoustic wave equation. They found that the method needs a low value of G (the number of grid points per minimum wavelength), close to that used by global pseudospectral methods, and that the accuracy is high and almost unchanged even for very long propagation distances. The method practically eliminates errors due to numerical dispersion, common in low order finite elements. A value of G=4.5, for example, is necessary when using polynomials of order N=8, compared with the values of G=15-30 needed by standard finite difference or finite element schemes (Marfurt, 1984).

2D Chebyshev Spectral Element Space

In first place, the approximating functional spaces must be constructed. To do this we decompose the original spatial domain into subdomains, and then, on each subdomain an approximating function is defined as a truncated expansion of Chebyshev polynomials. More specifically, in the case of two-dimensional problems, we decompose the original spatial domain Ω into non-overlapping quadrilateral elements Ω_e, where $e = 1, \ldots, n_e$, and n_e is the total number of elements. Here, we assume that the Euclidean space $\mathbb{R}^2$ is referred to an orthonormal system $\{0, \mathbf{e}_1, \mathbf{e}_2\}$, i.e. $\mathbf{x} = x_1\mathbf{e}_1 + x_2\mathbf{e}_2 = \{x_\alpha\}$, where $\mathbf{x}$ is the position vector on Ω. As approximating functions on each element Ω_e, we choose functions belonging to the $\mathbb{P}_{N_1}\otimes\mathbb{P}_{N_2}$ space i.e., polynomials of degree $\le N_1$ in x_1 and of degree $\le N_2$ in x_2. Then, a global approximating function is build up as a sum of the elemental approximating functions. This is, therefore, a continuous function which is a piecewise polynomial defined on the decomposition $\tilde{\Omega}$ of the original domain Ω. In our case, the polynomial space is constructed by using the Chebyshev orthogonal polynomials and for simplicity we assume $N_1 = N_2 = N$, i.e., the order of the polynomials is the same in the two directions x_1 and x_2.

It can be shown that a function $f(\xi) = f(\xi_1, \xi_2)$, defined on the square interval $[-1, 1] \times [-1, 1]$, can be approximated by a truncated expansion using a tensor product of Chebyshev polynomials as follows:

$$\tilde{f}(\xi) = \sum_{i=0}^{N}\sum_{j=0}^{N} \tilde{f}_{ij}\,\varphi_i(\xi_1)\varphi_j(\xi_2) = \sum_{i=0}^{N}\sum_{j=0}^{N} \tilde{f}_{ij}\,\phi_{ij}(\xi) \quad , \tag{1}$$

where $\tilde{f}_{ij} = f(\xi_{ij})$ are the grid values of the function f, and $\varphi_i(\xi) \in \mathbb{P}_N$ are Lagrangian interpolants satisfying the relation $\varphi_i(\xi_k) = \delta_{ik}$ within the interval $[-1, 1]$ and identically zero outside. Here δ_{ik} denotes the Kronecker-delta symbol and ξ stands for ξ_1 or ξ_2. The Lagrangian interpolants are given by

$$\varphi_i(\zeta) = \frac{2}{N}\sum_{p=0}^{N}{}'' \frac{1}{\bar{c}_i\bar{c}_p} T_p(\zeta_i)T_p(\zeta) \quad , \text{ with } \quad \bar{c}_i = \begin{cases} 1 & \text{for } i \neq 0, N \\ 2 & \text{for } i = 0, N \end{cases} , \tag{2}$$

where T_p are the Chebyshev polynomials and ζ_i are the Chebyshev Gauss-Lobatto quadrature points $\zeta_i = \cos(\pi i/N)$ for $i = 0, \ldots, N$. The coordinates $\xi_{ij} = \{\xi_{1i}, \xi_{2j}\}$ of the internal nodes for the discretization of the quadrilateral domain $[-1, 1] \times [-1, 1]$ are obtained as Cartesian products of the ζ_i points. In order to apply these interpolants and construct the approximating function space, we need to define the mapping $\Lambda^{(e)}(\mathbf{x}): \mathbf{x} \in \Omega_e \to \xi^{(e)} \in [-1, 1]^2$ between the points $\mathbf{x} \in [a_e, a_{e+1}] \times [b_e, b_{e+1}]$ of each element Ω_e of the decomposition $\tilde{\Omega}$ in the physical space and the local element coordinate system $\{\xi_1, \xi_2\}$ by

$$\Lambda^{(e)}(\mathbf{x}) \equiv \{\xi_1^{(e)}, \xi_2^{(e)}\} = \left\{ \frac{2}{\Delta_1^e}(x_1 - a_e) - 1 \ , \ \frac{2}{\Delta_2^e}(x_2 - b_e) - 1 \right\} , \tag{3}$$

with $\Delta_1^e = a_{e+1} - a_e$ and $\Delta_2^e = b_{e+1} - b_e$ dimensions of the element Ω_e. Then, the global approximating function is formed by the sum of the elemental approximating functions (1) defined on each element.

Two-dimensional Elastic Wave Equation

For a disturbance propagating in a bounded, inhomogeneous medium, the elastic field is described by the classical elastodynamic equation (e.g. Pilant, 1979). Let us denote by Ω a domain with boundary Γ and let us assume that Ω is an open, bounded and connected region of $\mathbb{R}^2$, and that Γ is a piecewise continuous curve where boundary conditions can be imposed. Furthermore, we denote by t the time variable defined over $[0, T]$ with $T > 0 \in \mathbb{R}$, and $\partial_\alpha \mathbf{u}$ as the partial derivative with respect to the variable x_α. Using the abbreviated subscript notation of acoustic, let us define the differential operator $\mathbf{D}$ as

$$\mathbf{D} = \begin{vmatrix} \partial_1 & 0 \\ 0 & \partial_2 \\ \partial_2 & \partial_1 \end{vmatrix} , \tag{4}$$

and $\sigma = \{\sigma_{11}, \sigma_{22}, \sigma_{12}\}^T$, $\varepsilon = \{\varepsilon_{11}, \varepsilon_{22}, 2\varepsilon_{12}\}^T$ (5)

the stress and the strain vectors respectively, and the superscript T denotes the transpose of a vector or a matrix. With these definitions the equation of motion becomes

$$\rho \frac{\partial^2 \mathbf{u}}{\partial t^2} - \mathbf{D}^T \sigma(\mathbf{u}) = \mathbf{f} , \tag{6}$$

where $\mathbf{u}(\mathbf{x},t)$ is the displacement field, $\mathbf{f}(\mathbf{x},t)$ are the body forces per unit volume in Ω, and ρ is the density. The stress-strain relation for a linear elastic and isotropic medium is given by

$$\sigma(\mathbf{u}) = \mathbf{C}\, \varepsilon(\mathbf{u}) , \tag{7}$$

where $\mathbf{C}$ is the elastic stiffness matrix

$$\mathbf{C} = \begin{vmatrix} \lambda + 2\mu & \lambda & 0 \\ \lambda & \lambda + 2\mu & 0 \\ 0 & 0 & \mu \end{vmatrix} , \tag{8}$$

and μ and λ are the Lame constants. The components of the strain vector ε are related to the displacement field by

$$\varepsilon(\mathbf{u}) = \mathbf{D}\, \mathbf{u} . \tag{9}$$

Equations (6) to (9), with suitable conditions specified on the boundaries and prescribed initial conditions for the elastic field, describe the propagation of compressional and shear waves in a two-dimensional inhomogeneous medium. If we look for sufficiently regular solutions $\mathbf{u}$, and no forces are imposed on the boundary Γ, an equivalent variational formulation of equation (6) is to find the solution $\mathbf{u}(\mathbf{x},t)$ of

$$\frac{d^2}{dt^2}(\mathbf{w}, \rho \mathbf{u})_\Omega + a(\mathbf{w}, \mathbf{u})_\Omega = (\mathbf{w}, \mathbf{f})_\Omega , \tag{10}$$

for all functions $\mathbf{w}(\mathbf{x})$ which vanish on the boundary Γ and which, together with their first derivatives, are square integrable over Ω. The quantities $a(\cdot,\cdot)_\Omega$ and $(\cdot,\cdot)_\Omega$ are symmetric, bilinear forms defined by

$$(\mathbf{w}, \rho \mathbf{u})_\Omega = \int_\Omega \rho\, \mathbf{w}^T \cdot \mathbf{u}\, d\Omega , \tag{11}$$

$$a(\mathbf{w}, \mathbf{u})_\Omega = \int_\Omega \varepsilon(\mathbf{w})^T \sigma(\mathbf{u})\, d\Omega = \int_\Omega \mathbf{w}^T \mathbf{D}^T \mathbf{C}\, \mathbf{D}\, \mathbf{u}\, d\Omega , \tag{12}$$

$$(\mathbf{w}, \mathbf{f})_\Omega = \int_\Omega \mathbf{w}^T \cdot \mathbf{f}\, d\Omega . \tag{13}$$

where equations (7) and (9) have been used.

SPEM method

In order to obtain the spectral-element approximation of equation (10), we decompose Ω into rectangular non-overlapping elements Ω_e, and on the decomposition $\bar{\Omega}$ we define the trial functions $\tilde{\mathbf{u}}(\mathbf{x},t)$ and the weight functions $\tilde{\mathbf{w}}(\mathbf{x})$ such that

$$\tilde{\mathbf{u}}(\mathbf{x},t) = \bigcup_{e=1}^{n_e} \tilde{\mathbf{u}}_e(\mathbf{x},t) , \qquad \tilde{\mathbf{w}}(\mathbf{x}) = \bigcup_{e=1}^{n_e} \tilde{\mathbf{w}}_e(\mathbf{x}), \tag{14}$$

where $\tilde{\mathbf{u}}_e$ and $\tilde{\mathbf{w}}_e$ denote the restriction to Ω_e of $\tilde{\mathbf{u}}$ and $\tilde{\mathbf{w}}$, respectively. According to the Galerkin approach, the functions $\tilde{\mathbf{u}}_e$ and $\tilde{\mathbf{w}}_e$ take the following form in the local coordinate system:

$$\tilde{\mathbf{u}}_e(\xi, t) = \sum_{i=0}^{N}\sum_{j=0}^{N} \tilde{\mathbf{u}}_e(\xi_{ij}^{(e)}, t)\, \phi_{ij}(\xi) , \quad \tilde{\mathbf{w}}_e(\xi) = \sum_{i=0}^{N}\sum_{j=0}^{N} \tilde{\mathbf{w}}_e(\xi_{ij}^{(e)})\, \phi_{ij}(\xi) , \tag{15}$$

where $\tilde{\mathbf{u}}_e(\xi_{ij}^{(e)}, t)$ and $\tilde{\mathbf{w}}_e(\xi_{ij}^{(e)})$ are the grid values of the unknown solution and of the weight functions, respectively. Using the approximating function spaces (14) to solve equation (10), it follows that the two-dimensional wave propagation problem is equivalent to finding $\tilde{\mathbf{u}}_e$ such that for all $\tilde{\mathbf{w}}_e$ the following equations are satisfied in each element Ω_e:

$$\frac{d^2}{dt^2}(\tilde{\mathbf{w}}_e, \rho \tilde{\mathbf{u}}_e)_N + a(\tilde{\mathbf{w}}_e, \tilde{\mathbf{u}}_e)_N = (\tilde{\mathbf{w}}_e, \tilde{f}_e)_N , \tag{16}$$

where $a(\cdot,\cdot)_N$ and $(\cdot,\cdot)_N$ are symmetric, bilinear forms computed according to the definitions (11-13) at the element level. Using the previous definition of $\varphi_i(\zeta)$ (eq. (2)), we can compute the derivative matrix $D_{ij} = d\varphi_i(\zeta_j)/d\zeta$ and then, the discrete differential operator

$$\mathbf{D}_{ij}^{(e)} = \sum_{k=0}^{N} \begin{vmatrix} D_{ik}\phi_{kj} & 0 \\ 0 & D_{jk}\phi_{ik} \\ D_{jk}\phi_{ik} & D_{ik}\phi_{kj} \end{vmatrix} . \tag{17}$$

We now apply the expansions (15) to the terms of equation (16) and evaluate the resulting elemental integrals using the mapping $\Lambda^{(e)}(\mathbf{x})$ and the discrete operator (17). Requiring that the variational equation be satisfied for all $\tilde{\mathbf{w}}_e$, the spectral element approximation of the original equation finally yields a set of linear equations

$$\mathbf{M}\, \ddot{U} + \mathbf{K}\, U = F , \tag{18}$$

with $U(0) = \{U_0\}$, $\dot{U}(0) = \{\dot{U}_0\}$ as initial conditions, where the unknown vector U contains the values of the discrete solution $\tilde{\mathbf{u}}$ at all Chebyshev points $x_{ij}^{(e)}$, for $i,j = 0, \ldots, N$ and for all $e = 0, \ldots, n_e$. A dot above a variable denotes differentiation with respect to the time. In equation (18), $\mathbf{M}$ is the mass matrix, $\mathbf{K}$ is the stiffness matrix, and F is the force vector obtained after a global nodal renumbering and assembly of all the elemental matrices and force vector contributions. They can be computed by using the following expressions:

$$\mathbf{M} = \sum_{e=1}^{n_e}{}' \mathbf{M}^{(e)} , \quad \mathbf{K} = \sum_{e=1}^{n_e}{}' \mathbf{K}^{(e)} \text{ and } F = \sum_{e=1}^{n_e}{}' F^{(e)} , \tag{19}$$

where Σ' denotes the matrix element summation or 'stiffness' summation over all the elements, and $\mathbf{M}^{(e)}$, $\mathbf{K}^{(e)}$ and $F^{(e)}$ are the elemental matrices and force vector, respectively. The contributions from nodes which are common to an element pair are summed to enforce the continuity requirement of the solution on the element boundaries. The elemental matrices and force vector are given by

$$\mathbf{M}^{(e)} = \left[\mathbf{M}_{ijlm}^{(e)}\right] , \quad \mathbf{M}_{ijlm}^{(e)} = \delta_{\alpha\beta} \int_{\Omega_e} \phi_{ij}\, \rho\, \phi_{lm}\, d\Omega , \tag{20}$$

$$\mathbf{K}^{(e)} = \left[\mathbf{K}_{ijlm}^{(e)}\right] , \quad \mathbf{K}_{ijlm}^{(e)} = \int_{\Omega_e} \mathbf{D}_{ij}^{(e)T} \mathbf{C}\, \mathbf{D}_{lm}^{(e)}\, d\Omega , \tag{21}$$

$$F^{(e)} = \left\{F_{ij}^{(e)}\right\} , \quad F_{ij}^{(e)} = \int_{\Omega_e} \phi_{ij}\, \mathbf{f}\, d\Omega , \tag{22}$$

where $\mathbf{M}_{ijlm}^{(e)}$, $\mathbf{K}_{ijlm}^{(e)}$, and $F_{ij}^{(e)}$ are the nodal submatrices and vector respectively. To solve the system of linear, second-order ODE with constant coefficients (18), we must integrate over the time interval $[0, T]$. This may be done by discretizing the time variable as $t_n = n\Delta t$, $0 \le n \le N_T$, where $\Delta t = T/N_T$, and N_T is the total number of time steps. The solution at time t_n, is $U_n = U(t_n)$. As time integration scheme we use the Newmark Constant Average Acceleration scheme , which is a two-step implicit algorithm, unconditionally stable and second-order accurate (Hughes, 1987). The solution at time t_{n+1} is obtained by solving the sparse, symmetric system of linear equations

$$\left(\mathbf{M} + \frac{\Delta t^2}{4}\mathbf{K}\right) U_{n+1} = \frac{\Delta t^2}{4} F_{n+1} + \mathbf{M}\left(U_n + \Delta t \dot{U}_n + \frac{\Delta t^2}{4} \ddot{U}_n\right) \tag{23}$$

with the Conjugated Gradient method preconditioned by the Incomplete Cholesky Factorization.

Numerical results

In order to check the accuracy of the algorithm, we compare analytical and numerical solutions for an impulsive point force acting in an elastic homogeneous medium (e.g., Pilant, 1979). The test model is shown in Figure 1, and consists of a square domain with side L = 1980 m , and velocities and density given by V_p = 3000 m/s , V_s = 1800 m/s , and ρ = 2400 kg/m³ , respectively. A vertical band-limited force is applied at point S, with time-history given by $f(t) = \exp[C(t-t_0)^2] \cos[2\pi f(t-t_0)]$, where t_0 = 0.0818 s , C = 1032, and f = 22 Hz. The cut-off frequency of this source is f_0 = 50 Hz . The domain is discretized in straight Chebyshev quadrangles of order N = 8 with a value of G = 4.8, according to Priolo and Seriani (1991). Therefore the model consists of 33x33 elements; the size of the elements and the minumum grid distance are Δ^e = 60 m , and Δx_{min} = 7.5 m , respectively. A time step Δt = 0.375 ms is chosen, to ensure accuracy.

Figure 2 displays a snap shot of $|\mathbf{u}|$ at time 0.036 s, where the P- and S-waves can be easily recognized., Figures 3a to 3d compare analytical and numerical seismograms recorded at stations G_1 , G_2 , and G_3 , as shown in Figure 1. The u_1 component at stations G_1 and G_3 are not displayed since they are identically zero. The agreement is excellent with a maximum error of nearly 1% for all the stations. Machine accuracy can be achieved by increasing the order of the polynomial.

A more realistic example is displayed in Figures 4a to 4d. The model consists of a surface layer with a steplike structure overlying a half-space. Free boundary conditions are imposed at the surface. The geometry and physical properties are shown in Figure 4a. A vertical point source, indicated by a star, is applied at the surface. Fig. 4a to 4c show snapshots of $|\mathbf{u}|$ at propagation times 0.024 s, 0.036 s, and 0.048 s, respectively, where the direct P- and S-waves can be easily identified. More interesting are the near-surface phenomena, which can be seen in Figures 4b and 4c in the form of Rayleigh waves (R). In particular, Figure 4b, shows that the Rayleigh wave splits into two at the step, one of them reflected back (R1), and the other travelling downwards (R2). This wave is partially converted into an S wave (R2S in fig 4c). Figures 4d and 4e show the vector field u in a zone around the step at times 0.036 s and 0.048 s, respectively. The vector representation enhances the comprehension of the particle motion: compressional waves (P), shear waves (S), and the retrograde motion of the interface waves can be easily identified. In particular, Figure 4e shows a S-wave front (S) travelling through the surface layer, followed by a pseudo-Stoneley wave (pSt) propagating along the solid-solid interface with a retrograde motion. The velocity of this interface wave lies between the velocity of the layer and the Rayleigh wave velocity of the half space.

Conclusions

The algorithm is highly accurate as shown by the comparison of the analytical and numerical solutions in a homogeneous elastic medium. In fact, by using Chebychev polynomials of order eight, the maximum error is less than one percent. However, machine accuracy can be reached by increasing the order of the polynomial. The model with surface topography shows that the modeling correctly describes the wave phenomena, in particular the Rayleigh waves interacting with the corner, and the Stoneley wave at the solid-solid interface. Waves in this type of structure are naturally simulated by the SPEM algorithm but require special treatments with other direct methods since the corner generates instabilities. The main drawback of the method at the present stage is that it is not highly efficient in terms of storage and computer time. However, these disadvantages can be solved, for instance, by computing the solution element by element. Additional improvements involve the generalization of the method to curved quadrangular elements in order to model curved interfaces, and its extension to the three-dimensional case.

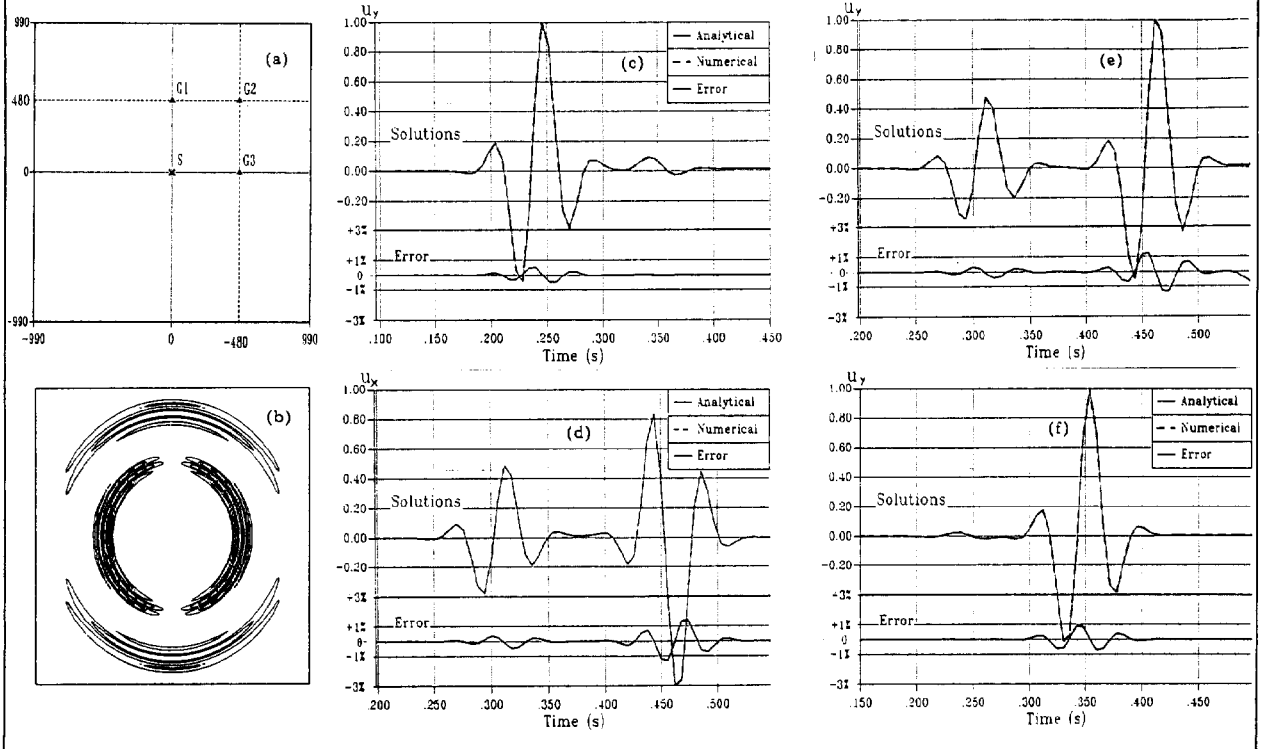

Fig. 1. Comparison between the analytical and numerical solutions for the response of a vertical force in an elastic homogeneous medium, (a) recording configuration, (b) snapshot of $|\mathbf{u}|$ at 0.036 s propagation time, (c) u_z component at G_1, (d) u_1 comp. at G_2, (e) u_2 comp. at G_2, and (f) u_2 comp. at G_3.

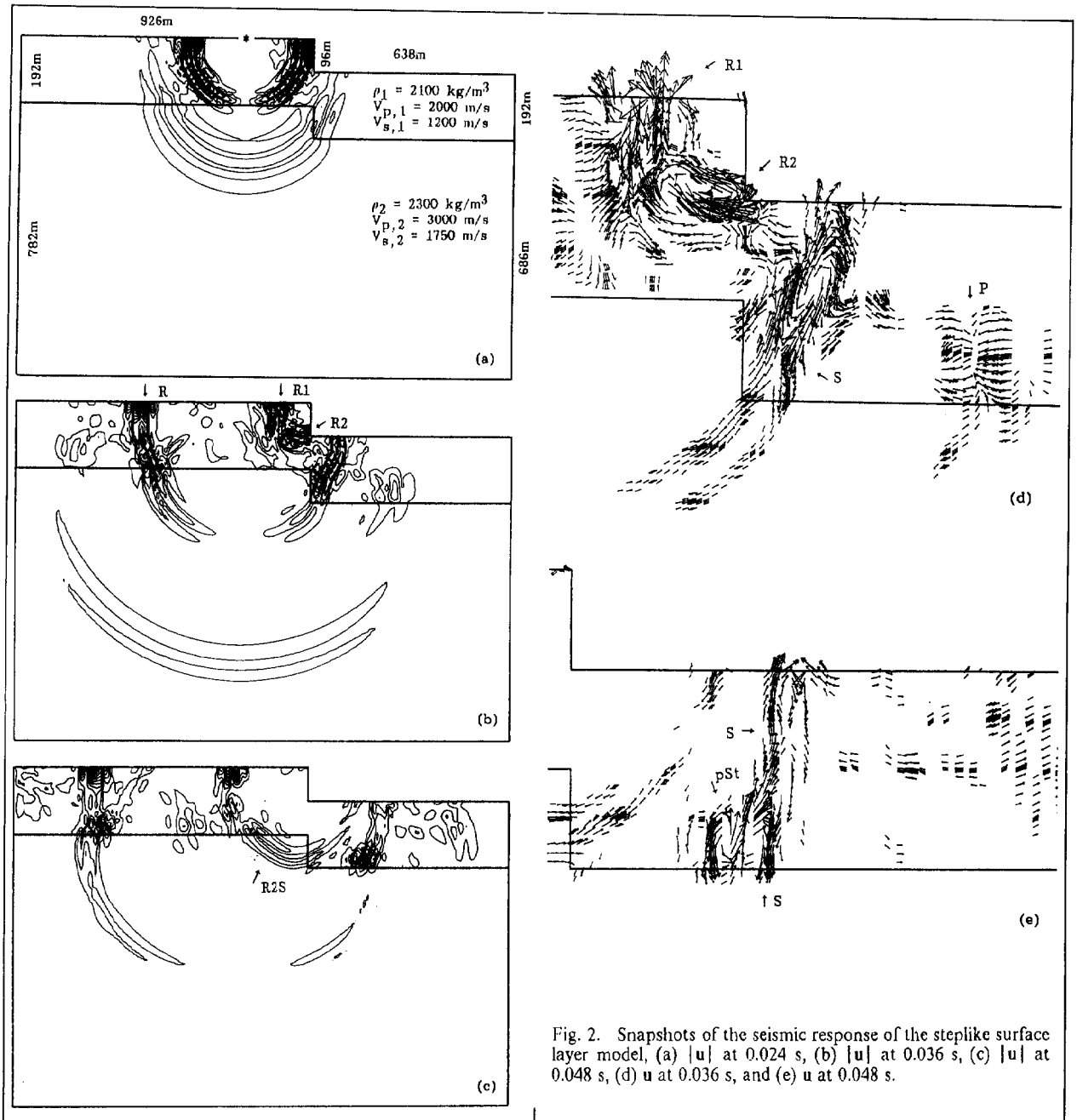

Fig. 2. Snapshots of the seismic response of the steplike surface layer model, (a) |u| at 0.024 s, (b) |u| at 0.036 s, (c) |u| at 0.048 s, (d) u at 0.036 s, and (e) u at 0.048 s.

Acknowledgements

This work was supported in part by the Commission of the European Communities under project EOS-1 (Exploration Oriented Seismic Modelling and Inversion), Contract N. JOUF-0033, as part of the GEOSCIENCE project within the framework of the JOULE R & D Programme (Section 3.1.1.b).

References

Hughes, T., 1987, "The finite element method", Prentice-Hall, New Jersey.

Marfurt, K.J., 1984, "Accuracy of Finite-Difference and Finite-Element Modeling of the Scalar and Elastic Wave Equations", Geophysics, 49, 533-549.

Patera, A.T., 1984, "A spectral element method for fluid dynamics: laminar flow in a channel expansion", J. of Comput. Physics, 54, 468-488.

Pilant, W. L., 1979, "Elastic Waves in the Earth", North-Holland, Amsterdam.

Priolo, E., Seriani, G., 1991, "A numerical investigation of Chebyshev spectral element method for acoustic wave propagation", Proc. of 13th IMACS World Congress on Computation and Applied Mathematics, Dublin, Ireland.

Seriani, G., Priolo, E., 1991, "High-Order Spectral Element Method for Acoustic Wave Modeling", 61st SEG Meeting, Houston (USA), Expanded Abstracts.